Ecotoxicology (2019) 28:175–188
https://doi.org/10.1007/s10646-018-2010-9

Influences of zinc oxide nanoparticles on *Allium cepa* root cells and the primary cause of phytotoxicity

Zhiqiang Sun[1] · Tiantian Xiong[1] · Ting Zhang[1] · Nanfang Wang[1] · Da Chen[2] · Shaoshan Li[1]

Accepted: 10 December 2018 / Published online: 5 January 2019

Abstract

Zinc oxide nanoparticles (ZnO-NPs) are widely used in consumer products, which have raised concerns about their impact on the human health and environment. In this study, *Allium cepa* were treated with 5 and 50 μg/mL ZnO-NPs solutions for 12, 24, and 36 h, respectively. The cytotoxic and genotoxic effects of ZnO-NPs in root meristems of *Allium cepa* cells were characterized by cell membrane integrity, metabolic activity, reactive oxygen species (ROS) accumulation, DNA damage, chromosome aberration, and cell cycle progression. Substantially elevated Zn levels were observed in the cytoplasmic and nuclear fractions, and the accumulation of zinc in the nuclear fraction (up to 9764 μg/g) was one magnitude greater than that in the cytoplasm (up to 541 μg/g). The complexation of Zn^{2+} with diethylene triamine pentacetic acid (DTPA) was performed to explicate the respective contribution of insoluble particles or Zn^{2+} to ZnO-NPs toxicity. We found that the inhibition of root growth accounted for 24.2% or 36.1% when the plants were exposed to Zn^{2+} that released from 5 or 50 μg/mL of ZnO-NPs for 36 h, respectively, whereas the exposure to 5 or 50 μg/mL of insoluble particles resulted in 75.8% or 63.9% of inhibition, respectively. These findings demonstrated that adverse effects exerted not just by Zn^{2+} released from ZnO-NPs, but also directly from the nanoparticles. These findings contribute to a better understanding of ZnO-NPs cytotoxicity and genotoxicity in plant cells and provide valuable information for further research on the phytotoxic mechanisms of ZnO-NPs.

Highlights

- Substantially elevated Zn levels were observed in the cytoplasmic and nuclear fractions of *A. cepa* roots.
- ZnO-NPs inhibited plant growth and induced severe cytotoxicity and genotoxicity.
- The toxicity of ZnO particles is higher than zinc ions released from them.

Keywords Zinc oxide nanoparticles · *Allium cepa* · DTPA · Phytotoxicity

Introduction

Nanoparticles (NPs) refers to materials in three-dimensional space of at least one dimension in the nanometer size (1–100 nm). Because of their specific characteristics, such as small size, high surface-to-volume ratio, and unique physical and chemical properties, the use of NPs in industrial and consumer products is fast increasing (Stampoulis et al. 2009). Among different nanomaterials, metal oxide (MO) NPs were subject to the greatest production and applications (Apel and Hirt 2004). These materials provided new solutions to long-persisting problems but cause unforeseen problems (Dev et al. 2018), prosperous industrial applications have enhanced the release of NPs into the

These authors contributed equally: Zhiqiang Sun, Tiantian Xiong

Supplementary information The online version of this article (https://doi.org/10.1007/s10646-018-2010-9) contains supplementary material, which is available to authorized users.

✉ Shaoshan Li
lishsh@scnu.edu.cn

[1] Key Laboratory of Ecology and Environmental Science in Guangdong Higher Education, School of Life Science, South China Normal University, 510631 Guangzhou, China

[2] School of Environment, Guangzhou Key Laboratory of Environmental Exposure and Health, and Guangdong Key Laboratory of Environmental Pollution and Health, Jinan University, 510632 Guangzhou, China

environment and subsequent exposure to ecosystems (Gottschalk et al. 2011).

Zinc oxide NPs (ZnO-NPs) are among the most commonly used NPs in a variety of applications such as personal care products, paints, and coating (Chang et al. 2012), the estimated global annual production of ZnO-NPs as of 2010 is >30,000 metric tons (Keller et al. 2013). Emissions during the manufacturing phase are estimated to be on the order 32–680 tons/year. For the use phase, the highest predicted emissions are from the use of ZnO-NPs in cosmetics, which are expected to pass through the wastewater treatment plants and then onto biosolids and effluent. Overall estimated emissions are 90–578 tons/year to the atmosphere, 170–2985 tons/year to receiving water bodies, and 3100–9283 tons/year to soils (Keller et al. 2013). As a result, the inappropriate handling, incidental and/or accidental release of NPs could result in serious environmental contamination (Dimkpa et al. 2012; Bandyopadhyay et al. 2015). A numerous reports have recently been published on the fate and toxicity of nanomaterials to terrestrial plants species (García-Gómez et al. 2017, 2018; Xiong et al. 2017; Rajput et al. 2018). A growing body of evidence has demonstrated that ZnO-NPs at a wide range of concentrations adversely affect plant growth of beet, tomato, green pea, maize, cucumber, rye, zucchini, and soybean, in a dose dependent manner (Lin and Xing 2007; Bandyopadhyay et al. 2015; García-Gómez et al. 2018). Zhang et al. (2015a) reported that the growth of *Schoenoplectus tabernaemontani* in the hydroponic mesocosms was significantly inhibited by ZnO-NPs (1000 mg/L) compared to a control. ZnO-NPs distribution in the root tissues of *Schoenoplectus tabernaemontani* was confirmed by scanning electron microscopy (SEM) (Zhang et al. 2015a). Lin et al. (2007) reported that ZnO-NPs greatly halted root elongation of ryegrass, radish, and rape. Authors also reported that ZnO-NPs adhered to the root surface of ryegrass, whereas high magnification transmission electron microscope (TEM) images showed the presence of NPs in the apoplast, cytoplasm, and nuclei of the endodermal cells and the vascular cylinder (Lin and Xing 2008). García-Gómez found significant Zn accumulation in bean (*Phaseolus vulgaris*) and tomato (*Solanum lycopersicon*) after ZnO-NPs applied to the soil, and NPs treatments altered the photosynthetic pigment concentration and induced oxidative stress in plants (García-Gómez et al. 2017).

Moreover, ZnO-NPs may also affect the plant cellular functions in various ways, which have been demonstrated in various plants, such as *Nicotiana tabacum, Allium cepa*, and *Vicia faba* (Ghosh et al. 2016; Dev et al. 2018). Their known cytotoxic effects include DNA damage (Venkatachalam et al. 2017), cellular internalization (Zhang et al. 2015a), reactive oxygen species (ROS) generation (Du et al. 2016), cell death (Kumari et al. 2011), cell-cycle arrest, and chromosome aberration (Ghosh et al. 2016). Although numerous reports have recently been published on the fate and toxicity of ZnO-NPs to terrestrial plants species, critical knowledge is still lacking. The main debates concerning their toxic modes of action is whether the toxicity of ZnO-NPs, as well as other oxide NPs, was caused by oxide NPs or the ions released from them (Xu et al. 2016; García-Gómez et al. 2017; Rajput et al. 2018). The known effect of dissolved zinc on the cells in the root tips have been largely studied, including inhibited plant growth (Bandyopadhyay et al. 2015; Zhang et al. 2015b) and altered the photosynthetic pigment concentration and induced oxidative stress in plants (García-Gómez et al. 2017). However, ZnO-NPs are nanosized and has high reactivity, the characteristic physiochemical properties of which is different from metal ions. Thus, the effects of ZnO-NPs (or metal ions released from NPs) in plants, especially the comprehensive study on the metal uptake, distribution and its cytotoxicity and genotoxicity are urgently needed.

In this work, we aimed to investigate the toxicity of ZnO-NPs by using the *Allium cepa* (*A. cepa*) model species. The *A. cepa* has been considered as an excellent biological model to study the toxicity of NPs (Ghosh et al. 2016). The *A. cepa* bioassay has been validated as an efficient and standard method for in situ monitoring of environmental substances by the United Nations Environment Programme (UNEP) and the International Programme on Chemical Safety (IPCS) (Grant 1982). Metal accumulation by *A. cepa* roots and distribution in the cytoplasmic and nuclear fractions were determined in the study. The effects of ZnO-NPs (or metal ions released from NPs) in root meristems of *A. cepa* cells were characterized by root growth, membrane integrity, chromosome aberration, metabolic activity, reactive oxygen species (ROS) accumulation, DNA damage, cell cycle arrest, and cell death. Specific objectives of our study were to: (1) evaluate the cytotoxic and genotoxic effects of ZnO-NPs on *A. cepa* roots; and (2) elucidate the respective contribution from metal ions released from ZnO-NPs or the particles themselves to the observed toxicity.

Materials and methods

Nanomaterial preparation

ZnO-NPs were purchased from Sigma-Aldrich®, USA (CAS #: 1314-13-2). Their particle sizes were less than 50 nm according to the manufacturer. The primary particle size analyzed by transmission electron microscope (TEM, JEM-2100 h Electron Microscope) is around 10–80 nm (Sup-Fig. 1 A, B), and the particle size distributions in ultrapure water are 180.6 and 201.7 nm for 5 and 50 µg/mL

ZnO-NPs, respectively (Sup-Fig. 1 C, D) (Malvern Nano ZSE). The zeta potential in ultrapure water for 5 and 50 µg/mL ZnO-NPs are −26 and −25.4 mV, respectively (Sup-Fig. 1 E, F). The specific area is 16.03 m^2/g according to the previous study of Goix et al. (2014). Stock solutions (1000 µg/mL, 50 mL) were prepared by suspending ZnO-NPs in ultrapure water, followed by sonication at 100 W and 30 kHZ (Ultrasonic cell crusher; SCIENTZ-IID; Ningbo; China) for 30 min and in coldness (Ghodake et al. 2011). Working solutions (5 or 50 µg/mL) were prepared by serial dilutions with ultrapure water, followed by 30 min of ultra-sonication.

Plant material and treatment condition

Healthy and equal-sized onion bulbs (average diameter 2.5 cm) was chosen for this study. The bulbs were cultured by immersing the root base into ultrapure water and grown at 27 °C until the root length reached approximately 2.0 cm. Onion roots were then treated with 5 and 50 µg/mL ZnO-NPs solutions (pH 6.8) for 12, 24, and 36 h, respectively. Ultrapure water was used as medium for control group (pH 6.8) (Qin et al. 2015). The experiments were carried out under natural illumination in a greenhouse with humidity of 65 ± 5%. Root length was measured every 12 h for each treatment and the morphology was observed. There was a total of six treatments, as well as a control group. Ten plants were used for each treatment.

Comparative study of the toxicity of ZnO-NPs suspension, Zn^{2+}, and insoluble particles

ZnO-NPs suspension was prepared at working concentrations of 5 and 50 µg/mL, and centrifuged at 16,000×*g* for 10 min to obtain ZnO-NP supernatant (Zn^{2+}). The concentrations of Zn^{2+} collected at 12, 24, and 36 h after preparation were determined by the flame atomic absorption spectrophotometric (AAS; Z-2300; Hitachi, Tokyo, Japan). In order to study the toxicity of particles, the zinc ions dissolved from ZnO-NPs were removed by diethylene triamine pentacetic acid (DTPA), which was used as an extracellular chelating agent for dissociating metal ions (Heim et al. 2015). To compare the toxicity of ZnO-NPs suspension, Zn^{2+}, and insoluble particles, the plants *A. cepa* were cultured in 10 different mediums, including ultrapure water (control), 0.03 µM DTPA, 5 and 50 µg/mL ZnO-NPs, 5 and 50 µg/mL ZnO-NP supernatant, 5 µg/mL ZnO-NPs + DTPA, 50 µg/mL ZnO-NPs + DTPA, 5 µg/mL ZnO-NP supernatant + DTPA, and 50 µg/mL ZnO-NP supernatant + DTPA. All treatments were conducted at pH of 6.8 and lasted for 36 h. Root length was measured every 12 h for each treatment and the morphology was observed.

Zn accumulation in plant roots and distribution in cytoplasmic and nuclear fractions

Zn concentration in plant roots were determined with following steps. Onion roots treated with 5 and 50 µg/mL ZnO-NPs solutions were harvested at 12, 24, and 36 h, respectively, and rinsed with tap water and then ultrapure water to clear away adhered ZnO-NPs from root surfaces. Then the root samples were oven-dried at 70 °C to a constant weight. Each sample (0.10 g dry weight [dw]) was digested with a 6-mL mixture of HNO_3/H_2O_2 (5:1 v/v) in a microwave oven (Model MDS-6, Preekem Scientific Instruments Co., Ltd., Shanghai, China). After digestion, samples were diluted to a volume of 10 mL with ultrapure water and then subjected to Zn analysis by AAS (Qiu et al. 2011). The recovery rates were within 80–86% and the detection limit for Zn is 0.002 mg/L.

To analyze Zn concentrations in cytoplasmic and nuclear fractions, the isolation of protoplasts was conducted according to Wang et al. (2015). Onion roots were placed in Petri dishes (1 g of root material per dish) containing 10 mL of washing buffer supplemented with 0.05% (w/v) BSA, 0.5 mM DTT, 2% (w/v) Cellulysin and 0.1% (w/v) pectolyase Y-23. Digestion of cell walls was carried out for 8 h at 25 °C with gentle shaking at 30 rpm. Ten milliliters of digested solution were filtered through a nylon mesh (114 µm) and rinsed twice with 5 mL of washing buffer. After purification, the protoplasts were prepared for extracting the nucleus fractions and cytoplasm as previously described (Heim et al. 2015). The collected protoplasts in advance was resuspended in 1.5 mL of hypotonic buffer (20 mM Tris–HCl, 10 mM NaCl, 3 mM $MgCl_2$; pH 7) including 60 µL DTT (0.5 mM) and incubated for 15 min on ice. Afterwards, 75 µL NP-40 detergent was added and mixed for 1 min. The homogenate was centrifuged at 4 °C at 1000×*g* for 10 min for separation of the cytoplasmic fraction (supernatant) and the nuclear fraction (pellet). Finally, plasma and nuclear fractions were filled up with ultrapure water to a total volume of 4 mL, and centrifuged at 4 °C and 16,000×*g* for 30 min. After removed the supernatant, the nucleus fractions and cytoplasm were oven-dried at 70 °C for 24 h and weighed. Each sample was digested with a 6-mL mixture of HNO_3/H_2O_2 (5:1 v/v) in a microwave oven, diluted to a volume of 10 mL with ultrapure water and subjected to Zn analysis with AAS.

Cytotoxicity (evaluation of cell membrane integrity and metabolic activity)

Cell membrane integrity was studied using the modified Evans blue staining method (Ghosh et al. 2015). Firstly, onion roots both in control and experimental group were stained with 0.25% (w/v) Evans blue solution for 15 min,

after washed with ultrapure water for 30 min, the roots were imaged for qualitative estimation of cell membrane integrity. Triton-X and heat-treated roots were used as positive control. For the quantitative estimation, 15 root tips with equal length (1 cm) were excised and immersed in 4 mL of *N, N*-dimethylformamide for 1 h at room temperature. The absorbance of Evans blue released was measured at 600 nm.

The cell metabolic activity was detected by 2,3,5-triphenyl tetrazolium chloride (TTC) staining (Ghosh et al. 2015). After ZnO-NPs treatment, 15 onion root tips were excised, immersed in 0.5% TTC, and then incubated at 35 ± 1 °C for 15 min in the darkness. Subsequently, the root tips were rinsed with distilled water and imaged (Nikon ECLLPSE 50i, Japan). Triton-X and heat-treated root were used as a positive control for the experiment. For the quantitative estimation, the colored complex triphenyl formazan was extracted from roots in 95% ethanol and the absorbance was recorded at 490 nm.

ROS generation

After 12 h of treatment, the roots from each treatment were selected and placed in tubes containing 5 mL tris buffer solution (pH 7.2) and 5 mL 2,7-dichlorodi-hydrofluorescein diacetate (DCFH-DA, 0.25 µM) solution. After 15 min treatment in DCFH-DA dye, the roots were thoroughly washed with tris buffer solution. The generation of ROS in roots was observed and imaged using a fluorescence microscope (Nikon Eclipse 50i, Japan) (Wang et al. 2015). The fluorescence intensity was quantified using the image processing and analysis software Image J 1.46r.

Genotoxicity (DNA damage, changes in cell mitosis and detection of cell cycle progression)

DNA damage in nuclei was determined using the comet assay previously described (Qin et al. 2015). Root tips from control and experimental groups were excised and immediately chopped with 500 mL precooled Galbraith's buffer (45 mM $MgCl_2 \cdot 6H_2O$, 30 mM $C_6H_5Na_3O_7 \cdot 2H_2O$, 20 mM 3-[N-morpholino] propanesulfonic acid, 0.1% [v/v] Triton X-100 [pH 7.0]), and then filtered through a 600 µm mesh sieve to acquire the nuclear suspension. Subsequently, 1% (w/v) low melting point agarose (60 mL) and nuclear suspension (40 mL) were mixed gently at 37 °C and laid on an microslide, which was previously prepared by dipping microslides into a solution of 1% (w/v) normal agarose gel and dried overnight at room temperature. A coverslip was placed on the mixture to obtain a uniform layer. The slides were allowed to solidify in darkness at 4 °C for 15 min. After that, the coverslips were removed and the slides were immersed in ice-cold lysing solution (2.5 M NaCl, 100 mM EDTA, 10 mM Tris–HCl and 1% [v/v] Triton X-100 [pH 10.0]), incubated in darkness at 4 °C for 15 min and electrophoresed at 4 °C for 30 min. After electrophoresis, the immunofluorescent specimens were examined under a fluorescence microscope (Nikon ECLIPSE 50i). The experiment was repeated three times with three slides per condition each time, and 30 randomly chosen comet images per slide were measured and analyzed using CASP software. The olive tail moment was calculated as a measure of DNA damage.

The changes in cell mitosis were observed according to the procedures outlined by Qin et al. (2015). Briefly, the fresh root tips in each treatment group were excised, every 12 h, respectively. Then were fixed with 95% ethanol and acetic acid (3:2) for 1 h, and hydrolyzed in a mixture of hydrochloric acid (1 M), ethanol (95%), and acetic acid (99.8%) (5:3:2) for 4 min at 60 °C. Subsequently, the root tips were squashed in carbol fuchsin solution examined using a Nikon ECLIPSE 50i microscope. Mitotic index (number of dividing cells per 1000 observed cells) was used for quantification.

To detect cell cycle progression, 30 *A. cepa* roots that treated with 5 or 50 µg/mL of ZnO-NPs solutions were harvested and minced in 1 mL of lysis buffer LB01 (15 mM Tris aminomethane, 2 mM Na_2EDTA, 0.5 mM spermine, 80 mM KCI, 20 mM NaCl, 15 mM mercapto ethanol, and 0.1% (v/v) Triton X-100, pH 7.5) (Ghosh et al. 2016). The suspension containing isolated nuclei was incubated with RNase (50 µg/mL) at 37 °C for 60 min, filtered through a 40 µm nylon mesh, and stained with propidium iodide solution (50 µg/mL) before detected by BD FACS Aria II flow cytometer (New Jersey, USA). A minimum of 20,000 events were recorded per concentration. The DNA content in the G0/G1, S, and G2/M phases were analyzed using FlowJo version 7.6 software (FlowJo, LLC, USA).

Statistical analysis

The statistical analyses were performed using SigmaPlot8.0 software. All data were presented as arithmetic mean ± standard error (SE). The significant difference between control and treated plants and among the treatments were evaluated by Student's *t*-test method and one way-ANOVA. The *r* values stand for the correlation coefficient between different parameters. The results were considered statistically significant at $p < 0.05$.

Results

Effects of ZnO-NPs suspension on *A. cepa* root length

The effects of ZnO-NPs suspension on *A. cepa* roots is shown in Fig. 1. Plant root length was varied with ZnO-NPs

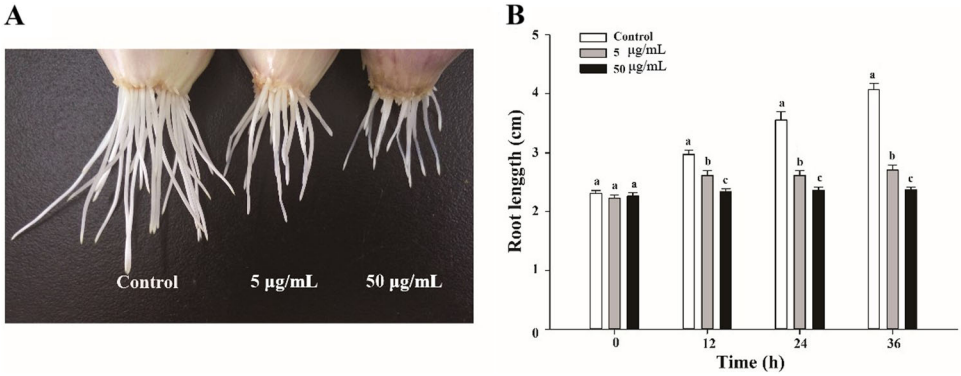

Fig. 1 Macroscopic effects of ZnO-NPs on root growth of *Allium cepa* (exposure for 36 h). **a** Effects of ZnO-NPs on root morphology. **b** Effects of ZnO-NPs on root growth. Values are expressed as the mean of three replicates for each treatment (±SE). Different letters indicate significant differences within each time group at $p < 0.05$

exposure concentration and time (Fig. 1). After 12, 24, and 36 h of exposure, ZnO-NPs significantly inhibited root growth at a concentration of 5 or 50 μg/mL when compared with controls ($p < 0.05$). The inhibition is more pronounced after plants treated with 50 μg/mL of ZnO-NPs. At the end of 36 h of exposure, *A. cepa* root tips in treatment groups (5 and 50 μg/mL ZnO-NPs) appeared to be swollen, soft, and friable, but the elongation region transparency was only observed in 50 μg/mL ZnO-NPs treatment group, where some roots were even broken (Fig. 1a). The length of root growth in the high concentration treatment group was only 0.1 cm on average during the entire experiment period. The results revealed that ZnO-NPs suspension significantly inhibited root growth and induced serious toxicity to *A. cepa*.

Comparison of the toxicity of ZnO-NPs suspension, Zn^{2+}, and insoluble particles

In the present study, Zn ions were removed by DTPA in order to compare the toxicity of insoluble particles solely with that induced by ions. The results indicated that DTPA had no effect on the growth of the *A. cepa* (Fig. 2a). The root length and morphological characteristics of *A. cepa* in the DTPA treatment group was the same as that in the control group. The effects of ZnO-NP supernatant (5 or 50 μg/mL) on *A. cepa* roots were observed, indicating that zinc ions dissociated from ZnO-NPs exhibited toxicity in *A. cepa* (Fig. 2b). After 24 or 36 h of exposure, ZnO-NP supernatant significantly inhibited root growth, especially in the treatment group of 50 μg/mL ZnO-NP supernatant, although the toxicity was lower than that induced by ZnO-NP suspension (Fig. 2b). The treatment of ZnO-NP supernatant with DTPA medium produced no significant effect on the root growth and morphology (Fig. 2c), indicating that DTPA could chelate most, if not all, of zinc ions and thereby prevent its inhibitory effect on plant growth. The removal of Zn ions from ZnO-NPs suspension lowered the overall toxicity of ZnO-NPs suspension (Fig. 2d), but the remaining suspension (mainly particles) still had very strong toxicity to *A. cepa* roots. This demonstrated that the toxicity was also partially attributed to the particles themselves. Quantitatively, the 36 h of exposure to Zn^{2+} released from 5 or 50 μg/mL of ZnO-NPs could result in an inhibition of 24.2% or 36.1% for root growth, respectively. By contrast, the exposure to 5 or 50 μg/mL of insoluble particles resulted in 75.8% or 63.9% of inhibition, respectively. These findings demonstrated that the toxicity induced by particles exceeded the effect by Zn^{2+}. In fact, the Zn^{2+} concentrations released from 5 and 50 μg/mL ZnO-NPs suspension were as low as 0.5–0.8 mg/L (Fig. 2e). In conclusion, the toxicity of ZnO-NPs suspension was attributed to both zinc ions and particles; the latter play a more important role.

Zn accumulation in roots and distribution in cells

There is a significant Zn accumulation in *A. cepa* roots and the accumulation was varied with ZnO-NPs concentration or exposure time (Fig. 3a). After 12 h of exposure, root Zn concentration reached 3181 or 9363 μg/g dw for 5 or 50 μg/mL ZnO-NPs treatment groups, respectively, significantly greater (61.6 and 181.4 times, respectively) than that in the control group ($p < 0.05$). After 24 h of exposure, root Zn concentration reached 4902.7 or 6205.03 μg/g dw for 5 or 50 μg/mL ZnO-NPs treatment groups, respectively, which are 75.48 and 95.6 times of that in the control group ($p < 0.05$). Metal concentration in plant root up to 5484.99 or 17785.3 μg/g dw for 5 or 50 μg/mL ZnO-NPs treatment groups, respectively, after 36 h of exposure. Zn concentrations were positively increased with the increasing ZnO-NPs concentration ($r = 0.949$, $p < 0.01$), and also positively correlated with exposure time ($r = 0.925$, $p < 0.01$). The differences in Zn concentrations between treatment and control groups also increased with increasing exposure time.

Our analysis of zinc distribution in cytoplasm and nuclei revealed that intracellular Zn-concentrations increased with ZnO-NPs concentration (Fig. 3b). Zn concentration in the nucleus was up to 9764 μg/g dw compared to that in the

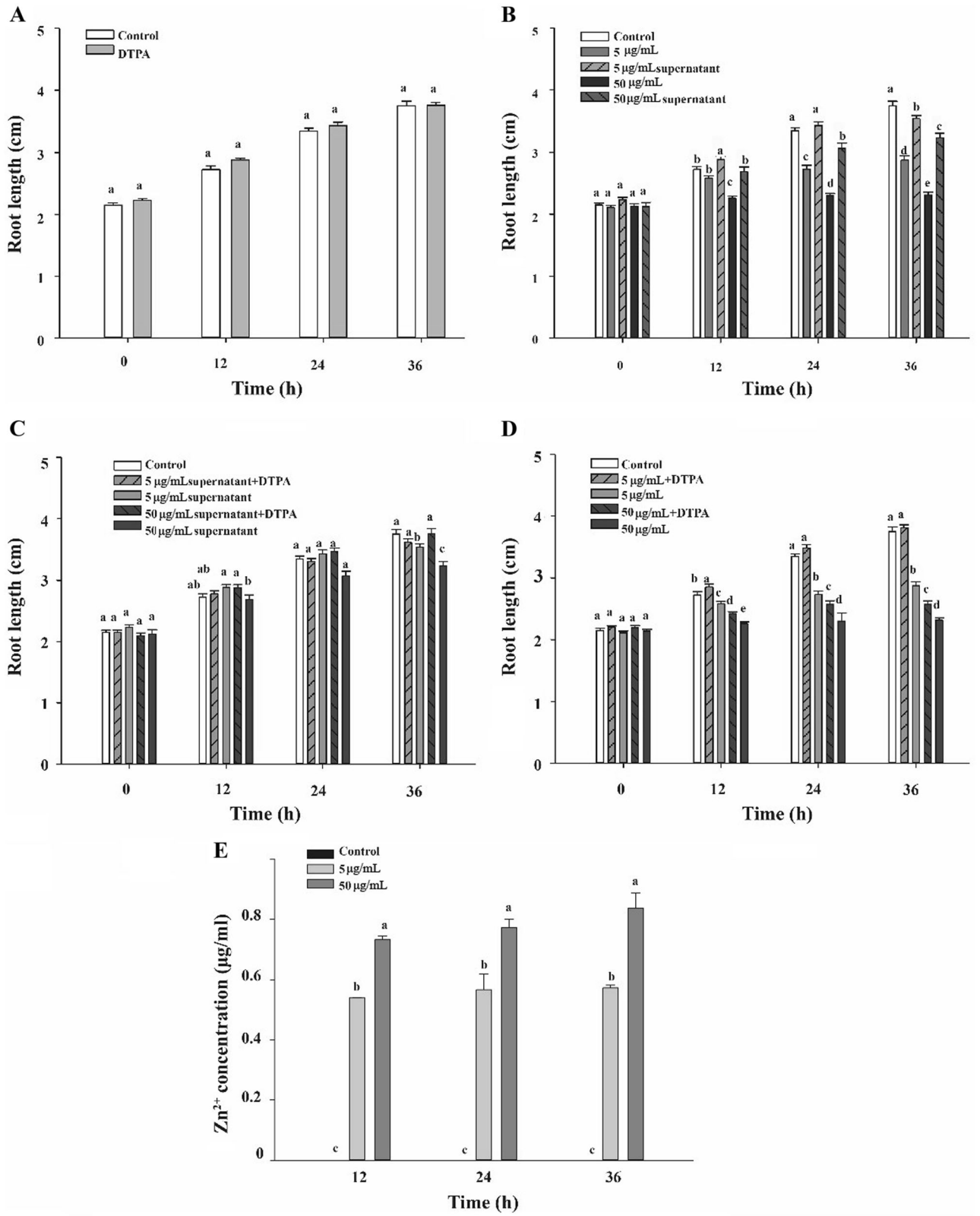

Fig. 2 Effects of **a** DTPA, **b** ZnO-NPs suspension and ZnO-NP supernatant, **c** ZnO-NP supernatant + DTPA, and **d** ZnO-NPs suspension + DTPA on roots growth of *Allium cepa*, and **e** Zn^{2+} concentration released from ZnO-NPs suspension. Values are expressed as the mean of three replicates for each treatment (±SE). Different letters indicate significant differences within each time group at $p < 0.05$

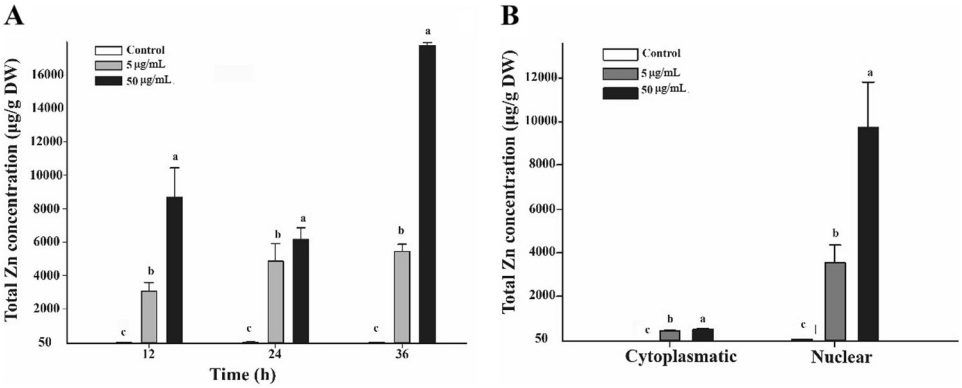

Fig. 3 Zn accumulation by *Allium cepa* roots **a** and distribution in cytoplasm and cell nucleus after 36 h of exposure **b** after treatment with different concentrations of ZnO-NPs. Values are expressed as the mean of three replicates for each treatment (±SE). Different letters indicate significant differences within each time group at $p < 0.05$

cytoplasm (up to 541 μg/g dw) after 36 h of ZnO-NPs treatment. The high metal concentration in the cytoplasm and nucleus could definitely induced cytotoxicity and genotoxicity to plants as confirmed in the following sections.

Cytotoxicity (effects on cell membrane integrity and metabolic activity)

The cytotoxic potential of ZnO-NPs in *A. cepa* root cells was assessed using multiple endpoints. Evans blue dye, a marker of membrane integrity, was used to study cytotoxic effects. As living cells cannot be dyed blue, cells without complete cell membrane are exposed to dye solution so as to be dyed blue. After exposure to ZnO-NPs, the *A cepa* roots were dyed blue but the colors varied with ZnO-NPs concentration or exposure time (Sup-Fig. 2A). The roots exposed to ZnO-NPs showed higher dye uptake compared to the control roots (Sup-Fig. 2C). In addition, the *A. cepa* root of treatment group appeared to be increasingly darker with the increase of ZnO-NPs concentration or exposure time, suggesting more root cells were damaged by ZnO-NPs. The results demonstrated that ZnO-NPs damaged cell membrane integrity of *A. cepa*.

During the TTC assay, after exposure to ZnO-NPs, the color intensity of *A. cepa* roots decreased with increasing ZnO-NPs concentration or exposure time (Sup-Fig. 2B), indicating a lower cell metabolic activity of *A. cepa* root. A minimum metabolism was observed after 12 h, compared to the highest cell metabolic activity in the control group. Furthermore, the detected OD value was consistent with the observed color change in *A. cepa* roots (Sup-Fig. 2D). Our results indicate that ZnO-NPs exposure may decrease the activity of the mitochondrial respiratory chain.

Oxidative stress

ROS generation after 12 h of ZnO-NPs treatments is presented in Fig. 4a and B. A significant increase ($p < 0.05$) in fluorescence intensity of DCFH was observed after 5 and 50 μg/mL of ZnO-NPs treatments (Fig. 4a), indicating intracellular ROS production. The ROS content of treatment group was much higher than that of the control group, and increased along with the concentration of ZnO-NPs (Fig. 4b). This confirmed that ZnO-NPs induced significant ROS production, which has a high potential of inducing serious oxidative stress.

Genotoxicity (induction of DNA damage, chromosome aberration, and effects on cell cycle progression)

The comet assay was performed in *A. cepa* root nuclei to estimate DNA damage at cell level (Fig. 4c, d). After 12 h ZnO-NPs exposure, we observed from the comet electrophoresis map that the low concentration treatment group showed obvious trailing phenomenon compared with the control group, and the tail became more apparent under the high concentration treatment or when exposed for a longer time. The results reveal significant increment of DNA fragmentation after ZnO-NPs treatment and thus serious DNA damage in *A. cepa* roots.

Elevated zinc accumulation in the cell nucleus may affect cell mitosis. The genotoxic effect of ZnO-NPs was evaluated on the basis of *A. cepa* test results (mitotic index, micronucleus, and chromosomal aberrations). The chromosomes of root tip cells from control group showed typical morphological and structural changes across the different stages of the cell cycle (Fig. 5a–d). The chromosome disorder, break, chromosome bridges, chromosome stickiness, chromosome ring, and micronucleus were observed after ZnO-NPs treatments (Fig. 5e–t). Moreover, Sup-Table 1 summarizes the mitotic index and chromosome aberration rate in the root meristem cells of *A. cepa*. Cells exposed to ZnO-NPs exhibited a lower mitotic index than that of control cells, and the mitotic index significantly decreased with the increasing concentrations of ZnO-NPs and the prolonged exposure duration. Moreover, ZnO-NPs treated roots exhibited a high frequency of various kinds of

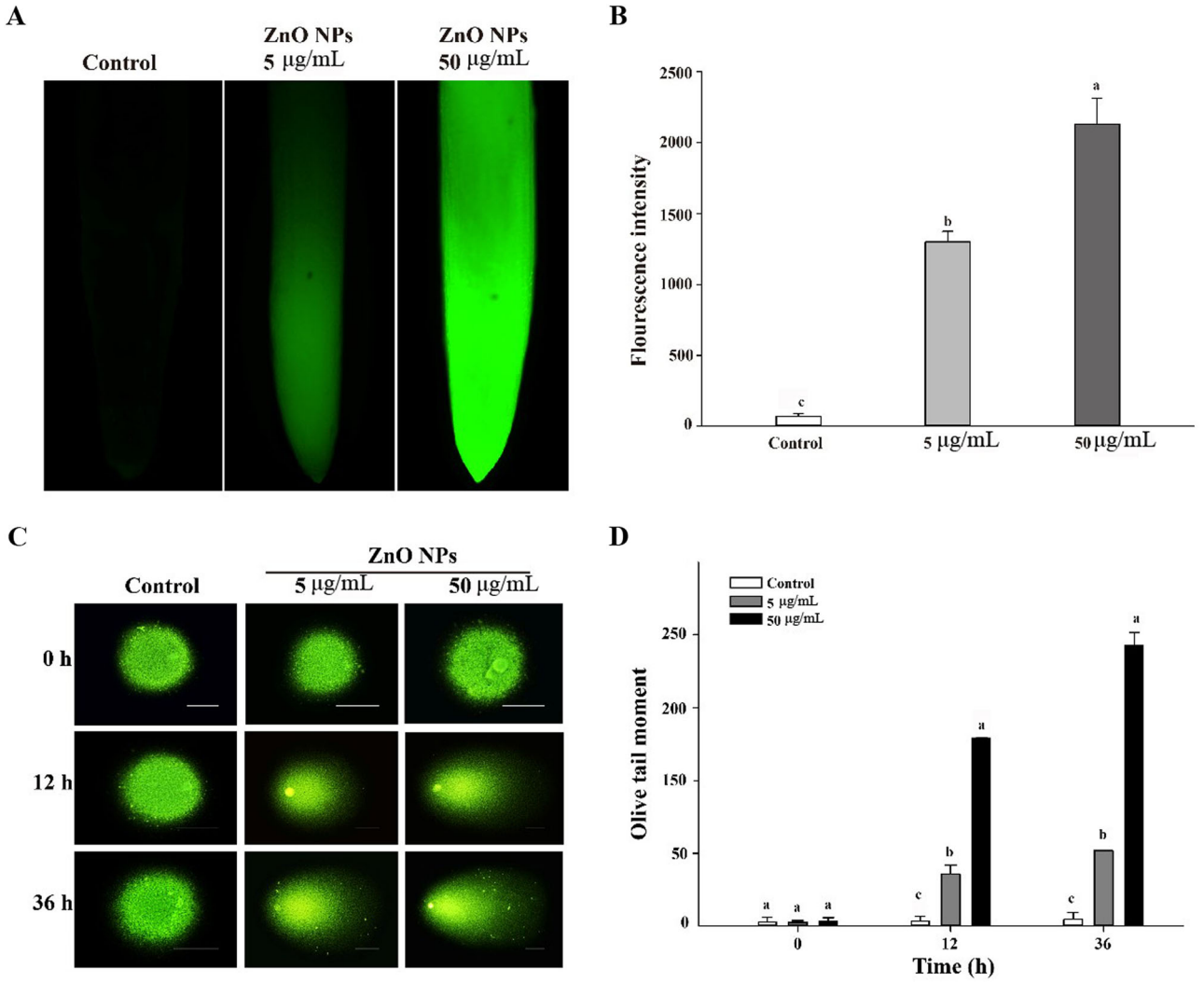

Fig. 4 ZnO-NPs-dependent reactive oxygen species (ROS) generation and DNA damage in root tip cells of *Allium cepa*. **a** Fluorescence images and **b** fluorescence intensity (12 h) of *A. cepa* roots in different treatment groups; **c** Fluorescence images of single-cell gel electrophoresis, scale bar = 50 μm; **d** The olive tail moment was calculated as a measure of DNA damage, values are expressed as mean ± SE ($n = 3$) and values with different letters differ significantly from each other within each time group ($p < 0.05$); Error bars represent standard errors

abnormalities. The chromosomal aberration rate increased progressively with the increase of exposure time or ZnO-NPs concentration. The frequency of chromosome stickiness was higher than that of the other abnormality types.

The effect of ZnO-NPs on cell cycle progression was studied on *A. cepa* root cells. The histogram obtained from the flow cytometry analysis revealed a significant ($p < 0.05$) decrease in G0/G1 and increase in S phase of peak values after ZnO-NPs exposure (Fig. 6a, b). The G2/M peak values showed no significant change when compared with the control. The histogram revealed that the S cell phase increased significantly with ZnO-NPs concentration, indicating that the ZnO-NPs probably caused the arrest of mitotic cells in the S phase. Since DNA replication occurs in the S phase, a great extent of DNA damage may affect the normal DNA replication after ZnO-NPs exposure.

Discussion

Effects of ZnO-NPs suspension on *A. cepa* root length

Our study revealed that ZnO-NPs suspension significantly inhibited root growth and induced serious toxicity to *A. cepa*, which is consistent with the findings from previous research. Previous studies demonstrated that ZnO-NPs mostly impacted plant growth, including in beet, tomato, green pea, maize, cucumber, rye, zucchini, and soybean (Bandyopadhyay et al. 2015; García-Gómez et al. 2018; Wang et al. 2018). According to Lin and Xing (2007), ZnO oxide nanoparticles were also shown to be inhibitive at root elongation, e.g. suspensions of 2000 mg/L nano-Zn or nano-ZnO practically terminated root elongation of the

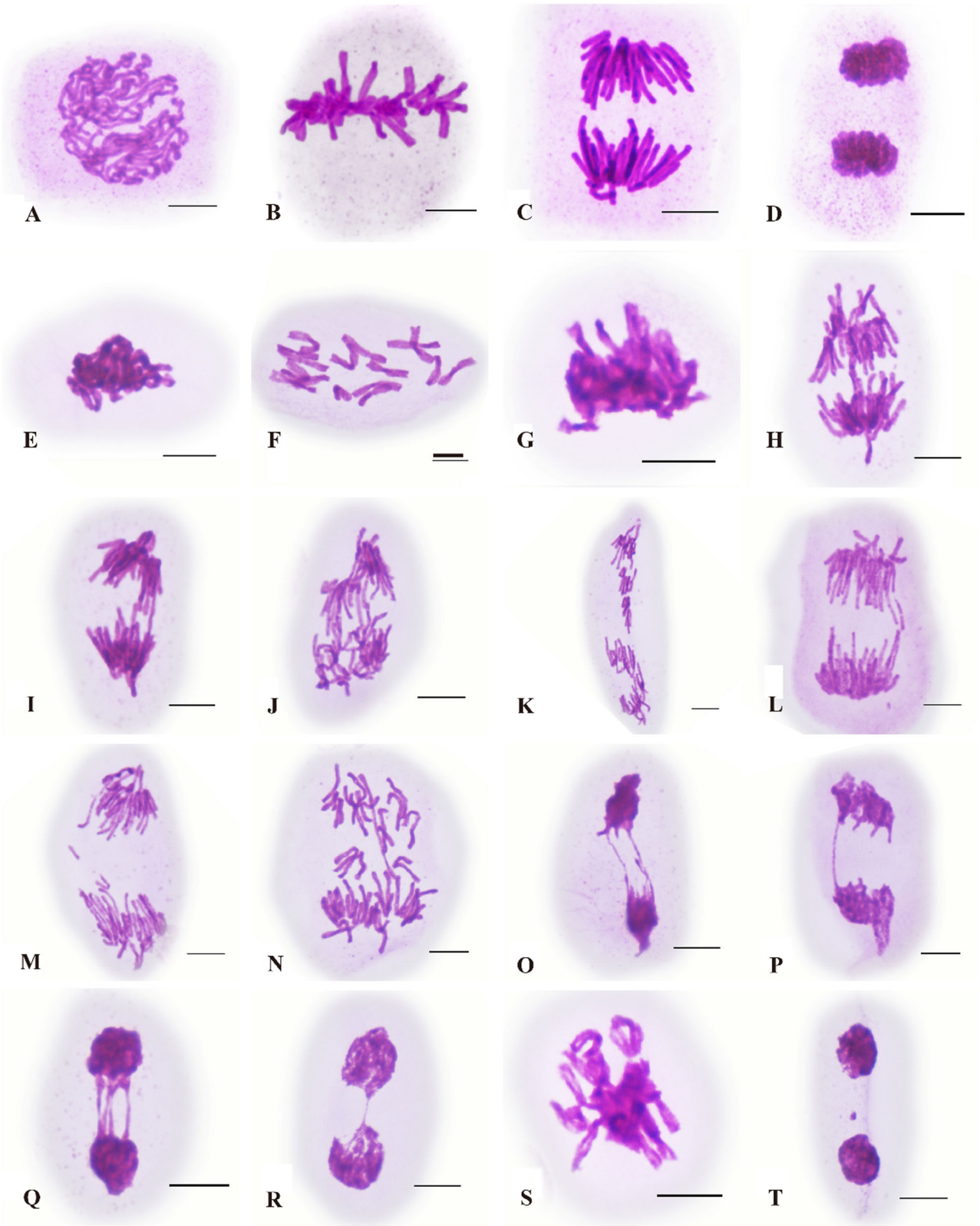

Fig. 5 Effects of ZnO-NPs on root meristem cell mitosis of *Allium cepa*. **a–d** Normal mitosis: **a** prophase, **b** metaphase, **c** anaphase, **d** telophase; **e–g** disturbed metaphase; **h–j** chromosome bridges; **k–m** chromosome breakage; **n** spindle breakage; **o–r** chromosome stickiness; **s** chromosome loop; **t** micronucleus. Scale bars = 10 μm

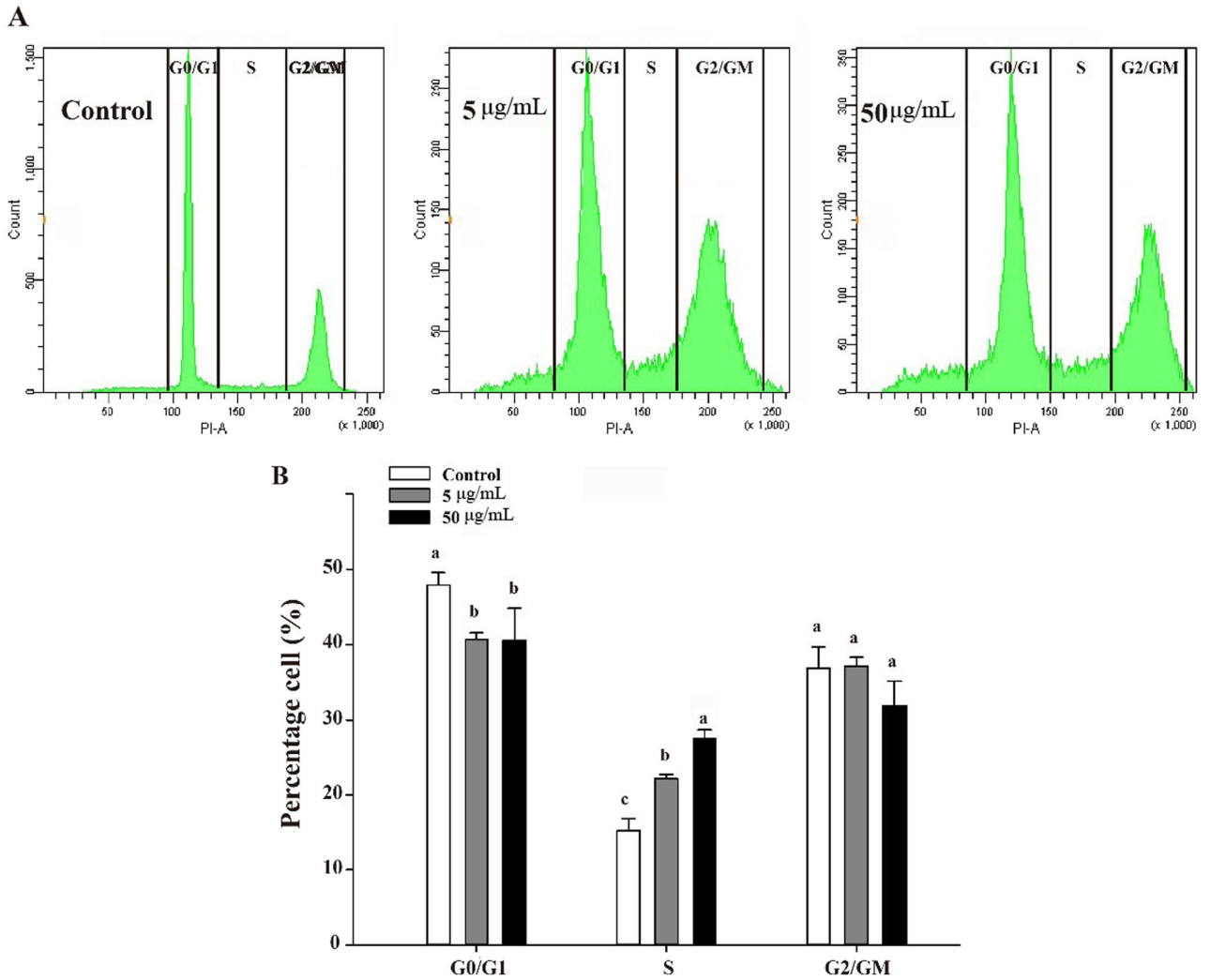

Fig. 6 Effect of ZnO-NPs on cell cycle progression of *Allium cepa* root cells. **a** Changes in cell cycle progression of different ZnO-NPs treatment groups obtained from flow cytometry; **b** The percentage of cell distribution in different phases of the cell cycle: G0/G1, S, and G2/M. Values are expressed as the mean of three replicates for each treatment (±SE). Different letters indicate significant differences within each time group at $p < 0.05$

tested plant species (radish, rape, ryegrass, lettuce, corn, and cucumber). Fifty percent inhibitory concentrations (IC50) of nano-Zn and nano-ZnO were estimated to be near 50 mg/L for radish, and about 20 mg/L for rape and ryegrass (Lin and Xing 2007). The root elongation of Chinese cabbage was severely inhibited by nano-ZnO when their seeds were soaked and incubated in a 40 mg/L nano-ZnO suspension for 72 h (Xiang et al. 2015). ZnO NPs at 1000 mg/L reduced root length of corn and cucumber by 17% ($p < 0.05$) and 51% ($p < 0.05$), respectively (Zhang et al. 2015a, 2015b). Moreover, the morphology changes of plant roots caused by high concentrations of ZnO nanoparticles (1000 mg/L) were also demonstrated by Lin and Xing (2008), the root tips of rye grass were shrank and epidermal and cortical cells were highly vacuolated and collapsed in the presence of high concentrations of ZnO. Our study derives analogical conclusion as previous report.

Comparison of the toxicity of ZnO-NPs suspension, Zn^{2+}, and insoluble particles

ZnO-NPs are prone to dissolve, but whether the toxicity of ZnO-NPs is caused by the released ions or the particles remains unclear (Lin et al. 2009). Some researchers attributed the toxicity to the dissolved ions from nanoparticles (Miao et al. 2009; Michaelis et al. 2017). However, Navarro et al. and Lubick suggested that the toxicity of nano-Ag to algae could not solely result from the released ions (Lubick 2008; Navarro et al. 2008); rather, the interaction of nanoparticles with algae also played an important role. Our study reveals that the toxicity of ZnO-NPs suspension was

attributed to both zinc ions and particles; the latter play a more important role. Similarly, the phytotoxicity of ZnO nanoparticles to *Arabidopsis* was also much stronger than solutions containing same concentration of soluble Zn (Lee et al. 2010). But according to the report of (Zhang et al. 2015a, 2015b), the toxicity of ZnO NPs (100, 1000 mg/L) on the root elongation of corn could be attributed to the nanoparticulate ZnO in comparison with Zn^{2+}, while released Zn ion from ZnO could solely contribute to the inhibition of root elongation of cucumber. Based on our study and the precious report, we speculate that the toxicity of ZnO-NPs could largely depended on the plant species.

Zn accumulation in roots and distribution in cells

Although Zn is an essential metal element, it can induce serious damage to plant growth and development when absorbed in large amounts (Wang et al. 2010). Previous studies found significant Zn accumulation and their potential phytotoxicity in plants such as *Zea mays* L., *Cucumis sativus* L., and *Brassica juncea* after ZnO exposure (Zhang et al. 2015a, 2015b).

Our study reveals a significant Zn accumulation by *A. cepa* roots and distribution in cytoplasm and cell nucleus after ZnO-NPs exposure. These results are consistent with the findings by Kumari et al. (2011), who noted that zinc oxide nanoparticles at 25, 50, or 100 μg/mL were internalized into *A. cepa* cells (Kumari et al. 2011). The internalization and distribution of zinc in cells is important to a better understanding of ZnO-NPs toxicity. The distribution of ZnO-NPs in the plant cells was also demonstrated by Lin and Xing (2008) and Zhang et al. (2015a, 2015b) by using the scanning electron microscopy and transmission electron microscopy analysis, their study revealed that ZnO could penetrate the cell walls and present within the plant cells (e.g. nucleus and cytoplasm) of *Lolium perenne* and *Schoenoplectus tabernaemontani*. Other type of nanoparticles, like TiO_2–nanoconjugates of 2.8 ± 1.4 nm in diameter, was also succeeded in root cell (*Arabidopsis thaliana*) penetration up to inside vacuoles and the nucleus (Kurepa et al. 2010).

Cytotoxicity (effects on cell membrane integrity and metabolic activity)

Evans blue dye was used as a marker of membrane integrity that living cells have the ability to exclude the dye at the plasma membrane, while the damaged cell is stained blue. Our results demonstrated that ZnO-NPs damaged cell membrane integrity of *A. cepa*; thus ZnO-NPs could easily enter into the cell, and subsequently affect plant growth (Ghosh et al. 2015). Consistent with the study of (Ghosh et al. 2015). who found a 3–4 fold increase in Evans blue uptake in *A. cepa* roots after exposed to multi-walled carbon nanotubes (10, 20, and 50 μg/mL).

Our results of DTT assay indicate that ZnO-NPs exposure may decrease the activity of the mitochondrial respiratory chain. Lower energy metabolism will affect many aspects of cells, such as cell growth, division, and DNA repair, which is hazardous for the growth of the *A. cepa* roots.

Oxidative stress

The ROS represents a group of free radicals, reactive molecules, and ions that are derived from O_2 (Apel and Hirt 2004). It is well recognized for dual roles as both beneficial and harmful factors, depending on their concentrations in plants. At a low concentration, ROS involves in signal transduction and mediates the regulation of cellular metabolic activity in plant cells, whereas at a high concentration it triggers oxidative damage to biomolecules and even cell death (Aaron et al. 2014).

The present study confirmed that ZnO-NPs induced significant ROS production, which could be positively correlated with the effects including H_2O_2 production, lipid per-oxidation, and even DNA damage (Sharma and Dietz 2009). ROS accumulation in cells can result in rapidly oxidation of normal biological macromolecules, such as nucleic acids, proteins, and lipids (Reddy et al. 2005; Yadav 2010). These attacks can cause irreparable metabolic disorder and cell death (Xiong et al. 2007). Thus, in the present study, ROS generation is considered to be one of the primary mechanisms of toxicity.

Genotoxicity (Induction of DNA damage, chromosome aberration and effects on cell cycle progression)

The results of comet assay reveal significant increment of DNA fragmentation after ZnO-NPs treatment and thus serious DNA damage in *A. cepa* roots. These results agree with that reported by Balasubramanyam et al. (2009), where DNA damage by ZnO-NPs was also observed. Zinc internalization, which accumulated in cell nucleus, and ROS generation could seriously affect the stability of nucleic acid (Qiu and Wang et al. 2011), and led to DNA damage in our study. Gichner et al. (2008) demonstrated that the incomplete excision repair sites were a source of DNA strand breaks detected in the comet assay. Rodriguez et al. (2011) indicated that DNA damage had a negative impact on cell mitosis and might lead to genomic instability and mutation. Based on the results of the comet assay, we conclude that ZnO-NPs has high potential of interacting with DNA and causing DNA damage in *A. cepa* root meristem cells.

Elevated zinc accumulation in the cell nucleus affected cell mitosis, including chromosome disorder, break, chromosome bridges, chromosome stickiness, chromosome ring, and micronucleus. Among these distortions, adhesion distortion is one of the most common types and induces high toxicity to cells. Adhesion distortion cannot be reversed and is very likely to cause cell death (Liu et al. 1992). Chromosome adhesion formation might be caused by change of physical and chemical properties of proteins in the chromosome (Patil and Bhat 1992). Previous studies also reported that ZnO-NPs was associated with the disturbance of mitosis (Kumari et al. 2011; Shaymurat et al. 2012). Rodríguez-Vargas et al. (2012) proved that DNA damage had a negative impact on cell mitosis. Maluszynska and Juchimiuk reported that chromosomal aberrations were the consequence of DNA double strand breaks that were unrepaired or repaired improperly (Maluszynska and Juchimiuk 2005).

Previous studies suggested that ZnO-NPs induced DNA damage and chromosomal aberrations, both of which influence DNA replication. In proliferating cells, DNA damage delays normal cell cycle progression by a complex network of responses. DNA damage following ZnO exposure may induce the arrest of cells at specific checkpoints. The study of cell cycle progression revealed that the S cell phase increased significantly with ZnO-NPs concentration, indicating that the ZnO-NPs probably caused the arrest of mitotic cells in the S phase. Since DNA replication occurs in the S phase, a great extent of DNA damage may affect the normal DNA replication after ZnO-NPs exposure.

These studies indicate that ZnO-NPs can induce DNA damage, affect the structural integrity of chromosomes, and result in the abnormal cell mitosis, and finally root growth inhibition.

According to our study, the potential mechanism of cytotoxicity and genotoxicity induced by ZnO-NPs were summarized as follows. ZnO-NPs adhered to the root surface of *A. cepa*, significantly accumulated by *A. cepa* root cells and distributed in cytoplasm and cell nucleus. Membrane integrity loss and reduced metabolic activity occurred in the treated cells. Moreover, the chromosome aberration, DNA damage, and cell-cycle arrest were noted. These changes might be attributed to the increase in ROS levels, which might have exceeded the scavenging ability of antioxidant enzymes. ZnO-NPs impaired the root morphology and the extra- and intra-cellular structure, increased oxidative stress and thus inhibited root growth and metabolic activity.

Conclusions

This study reveals a significant Zn accumulation by *A. cepa* roots and distribution in cytoplasm and cell nucleus after ZnO-NPs exposure. Our findings provide evidence for ZnO-NPs toxicity, characterized by root growth inhibition, loss of membrane integrity, decreased metabolic activity, ROS generation, chromosome aberration, DNA damage, cell-cycle arrest, and cell death in *A. cepa* roots. The results demonstrated that the toxicity of ZnO-NPs suspension was attributed to both zinc ions and particles and the latter was more important in the toxic effects. These findings contribute to a better understanding of ZnO-NPs cytotoxicity and genotoxicity in plant cells and provide valuable information for further research on the phytotoxic mechanisms of ZnO-NPs.

Acknowledgements This research was supported by the National Natural Science Foundation of China (Grant no. 31670266), the Guangdong Pearl River Scholar Funded Scheme (2012), the Science and Technology Program of Guangzhou, China (Grant no. 2014J4100053), and the Natural Science Foundation of Guangdong Province, China (Grant no. 2017A030313115) to Prof. Shaoshan Li. This work also received support from the Natural Science Foundation of China (Grant no. 41701572) and the Chinese Postdoctoral Science Foundation (Grant no. 2017M612684).

Compliance with ethical standards

Conflict of interest The authors declare that they have no conflict of interest.

Ethical approval This article does not contain any studies with human participants or animals performed by any of the authors.

References

Aaron B, Ron M, Nobuhiro S (2014) ROS as key players in plant stress signalling. J Exp Bot 65(5):1229–1240

Apel K, Hirt H (2004) Reactive oxygen species: metabolism, oxidative stress, and signal transduction. Annu Rev Plant Biol 55 (1):373–399

Balasubramanyam A, Sailaja N, Mahboob M, Rahman MF, Hussain SM, Grover P (2009) In vivo genotoxicity assessment of aluminium oxide nanomaterials in rat peripheral blood cells using the comet assay and micronucleus test. Mutagenesis 24(3):245–251

Bandyopadhyay S, Plascencia-villa G, Mukherjee A, Rico CM (2015) Comparative phytotoxicity of ZnO NPs, bulk ZnO, and ionic zinc onto the alfalfa plants symbiotically associated with *Sinorhizobium meliloti* in soil. Sci Total Environ 515–516:60–69

Chang YN, Zhang M, Xia L, Zhang J, Xing G (2012) The toxic effects and mechanisms of CuO and ZnO nanoparticles. Materials 5 (12):2850–2871

Dimkpa CO, McLean JE, Latta DE, Manangon E, Britt DW, Johnson WP, Boyanov MI, Anderson AJ (2012) CuO and ZnO nanoparticles: Phytotoxicity, metal speciation, and induction of oxidative stress in sand-grownwheat. Journal of Nanoparticle Research 14(9):1125

Dev A, Srivastava AK, Karmakar S (2018) Nanomaterial toxicity for plants. Environ Chem Lett 16:85–100

Dimkpa CO, McLean JE, Latta DE, Manangon E, Britt DW, Johnson WP, Boyanov MI, Anderson AJ (2012) CuO and ZnO

nanoparticles: Phytotoxicity, metal speciation, and induction of oxidative stress in sand-grown wheat. Journal of Nanoparticle Research 14(9):1125. https://doi.org/10.1007/s11051-012-1125-9

Du W, Tan W, Peralta-Videa JR, Gardea-Torresdey JL, Ji R, Yin Y, Guo H (2016) Interaction of metal oxide nanoparticles with higher terrestrial plants: physiological and biochemical aspects. Plant Physiol Biochem 110:210–225

García-Gómez C, Obrador A, González D, Babín M, Fernández MD (2017) Comparative effect of ZnO NPs, ZnO bulk and $ZnSO_4$ in the antioxidant defences of two plant species growing in two agricultural soils under greenhouse conditions. Sci Total Environ 589:11–24

García-Gómez C, Obrador A, González D, Babín M, Fernández MD (2018) Comparative study of the phytotoxicity of ZnO nanoparticles and Zn accumulation in nine crops grown in a calcareous soil and an acidic soil. Sci Total Environ 644:770–780

Ghodake G, Seo YD, Lee DS (2011) Hazardous phytotoxic nature of cobalt and zinc oxide nanoparticles assessed using *Allium cepa*. J Hazard Mater 186(1):952–955

Ghosh M, Bhadra S, Adegoke A, Bandyopadhyay M, Mukherjee A (2015) MWCNT uptake in *Allium cepa* root cells induces cytotoxic and genotoxic responses and results in DNA hypermethylation. Mutat Res 774:49–58

Ghosh M, Jana A, Sinha S, Jothiramajayam M, Nag A, Chakraborty A, Mukherjee A, Mukherjee A (2016) Effects of ZnO nanoparticles in plants: cytotoxicity, genotoxicity, deregulation of antioxidant defenses, and cell-cycle arrest. Mutat Res/Genet Toxicol Environ Mutagen 807:25–32

Gichner T, Patková Z, Száková J, Žnidar I, Mukherjee A (2008) DNA damage in potato plants induced by cadmium, ethyl methanesulphonate and γ-rays. Environ Exp Bot 62(2):113–119

Goix S, Lévêque T, Xiong TT, Schreck E, Baeza-Squiban A, Geret F, Uzu G, Austruy A, Dumat C (2014) Environmental and health impacts of fine and ultrafine metallic particles: assessment of threat scores. Environ Res 133:185–194

Gottschalk F, Ort C, Scholz RW, Nowack B (2011) Engineered nanomaterials in rivers--exposure scenarios for Switzerland at high spatial and temporal resolution. Environ Pollut 159 (12):3439–3445

Grant WF (1982) Chromosome aberration assays in Allium. A report of the U.S. Environmental Protection Agency Gene-Tox Program. Mutat Res/Fundam Mol Mech Mutagen 99(3):273–291

Heim J, Felder E, Tahir MN, Kaltbeitzel A, Heinrich UR, Brochhausen C, Mailänder V, Tremel W, Brieger J (2015) Genotoxic effects of zinc oxide nanoparticles. Nanoscale 7(19):8931–8938

Keller AA, McFerran S, Lazareva A, Suh S (2013) Global life cycle releases of engineered nanomaterials. J Nanopart Res 15:1692

Kumari M, Khan SS, Pakrashi S, Mukherjee A, Chandrasekaran N (2011) Cytogenetic and genotoxic effects of zinc oxide nanoparticles on root cells of *Allium cepa*. J Hazard Mater 190 (1–3):613–621

Kurepa J, Paunesku T, Vogt S, Arora H, Rabatic BM, Lu J, Wanzer MB, Woloschak GE, Smalle JA (2010) Uptake and distribution of ultrasmall anatase TiO_2 alizarin red s nanoconjugates in Arabidopsis thaliana. Nano Letters 10(7):2296–2302

Lee WL, Mahendra S, Zodrow K, Li D, Tsai YC, Braam J, Alvarez PJJ (2010) Developmental phytotoxicity ofmetal oxide nanoparticles to Arabidopsis thaliana. Environmental Toxicology and Chemistry 29(3):669–675

Lin D, Xing B (2007) Phytotoxicity of nanoparticles: inhibition of seed germination and root growth. Environ Pollut 150(2):243–250

Lin D, Xing B (2008) Root uptake and phytotoxicity of ZnO nanoparticles. Environ Sci Technol 42(15):5580–5585

Lin DH, Jing JI, Tian XL, Liu N, Yang K, Fengchang WU, Wang ZYA (2009) Environmental behavior and toxicity of engineered nanomaterials. Chin J 54(23):3590–3604

Liu D, Jiang W, Maoxie LI (1992) Effects of trivalent and hexavalent chromium on root growth and cell division of *Allium cepa*. Hereditas 117(1):23–29

Lubick N (2008) Nanosilver toxicity: ions, nanoparticles—or both? Environ Sci Technol 42(23):8617–8617

Maluszynska J, Juchimiuk J (2005) Plant genotoxicity: a molecular cytogenetic approach in plant bioassays. Arch Ind Hyg Toxicol 56(2):177–184

Miao AJ, Schwehr KA, Xu C, Zhang SJ, Luo Z, Quigg A, Santschi PH (2009) The algal toxicity of silver engineered nanoparticles and detoxification by exopolymeric substances. Environ Pollut 157 (11):3034–3041

Michaelis M, Fischer C, Colombi Ciacchi L, Luttge A (2017) Variability of zinc oxide dissolution rates. Environ Sci Technol 51 (8):4297–4305

Navarro E, Piccapietra F, Wagner B, Marconi F, Kaegi R, Odzak N, Sigg L, Behra R (2008) Toxicity of silver nanoparticles to *Chlamydomonas reinhardtii*. Environ Sci Technol 42 (23):8959–8964

Patil BC, Bhat GI (1992) A comparative study of MH and EMS in the induction of chromosomal aberrations on lateral root meris*tem in Clitoria ternatea L.* Bus Inf Syst Eng 2(4):249–258

Qin R, Wang C, Chen D, Björn LO, Li S (2015) Copper-induced root growth inhibition of *Allium cepa var. agrogarum L.* involves disturbances in cell division and DNA damage. Environ Toxicol Chem 34(5):1045–1055

Qiu Q, Wang Y, Yang Z, Xin J, Yuan J, Wang J, Xin G (2011) Responses of different chinese flowering cabbage (*Brassica parachinensis L.*) cultivars to cadmium and lead stress: screening for Cd+Pb pollution-safe cultivars. CLEAN - Soil Air Water 39 (11):925–932

Rajput VD, Minkina TM, Behal A, Sushkova SN, Mandzhieva S, Singh R, Gorovtsov A, Tsitsuashvili VS, Purvis WO, Ghazaryan KA, Movsesyan HS (2018) Effects of zinc-oxide nanoparticles on soil, plants, animals and soil organisms: a review. Environ Nanotechnol Monit Manag 9:76–84

Reddy AM, Kumar SG, Jyothsnakumari G, Thimmanaik S, Sudhakar C (2005) Lead induced changes in antioxidant metabolism of horsegram (*Macrotyloma uniflorum (Lam.) Verdc.*) and bengalgram (*Cicer arietinum L.*). Chemosphere 60(1):97–104

Rodriguez E, Azevedo R, Fernandes P, Santos C (2011) Cr(vi) induces DNA damage, cell cycle arrest and polyploidization: a flow cytometric and comet assay study in/r Pisum sativum. Chemical Research in Toxicology 24(7):1040–1047

Rodríguez-Vargas JM, Ruiz-Magaña MJ, Ruiz-Ruiz C, Majuelos-Melguizo J, Peralta-Leal A, Rodríguez MI, Muñoz-Gámez JA, De Almodóvar MR, Siles E, Rivas AL, Jäättela M, Oliver FJ (2012) ROS-induced DNA damage and PARP-1 are required for optimal induction of starvation-induced autophagy. Cell Research 22(7):1181–1198

Sharma SS, Dietz KJ (2009) The relationship between metal toxicity and cellular redox imbalance. Trends Plant Sci 14(1):43–50

Shaymurat T, Gu J, Xu C, Yang Z, Zhao Q, Liu Y, Liu Y (2012) Phytotoxic and genotoxic effects of ZnOnanoparticles on garlic (Allium sativum L.): A morphological study. Nanotoxicology 6 (3):241–248

Stampoulis D, Sinha SK, White JC (2009) Assay-dependent phytotoxicity of nanoparticles to plants. Environ Sci Technol 43 (24):9473–9479

Venkatachalam P, Jayaraj M, Manikandan R, Geetha N, Rene ER, Sharma NC, Sahi SV (2017) Zinc oxide nanoparticles (ZnONPs) alleviate heavy metal-induced toxicity in *Leucaena leucocephala* seedlings: a physiochemical analysis. Plant Physiol Biochem 110:59–69

Wang F, Jing X, Adams CA, Shi Z, Sun Y (2018) Decreased ZnO nanoparticle phytotoxicity to maize by arbuscular mycorrhizal

fungus and organic phosphorus. Environ Sci Pollut Res 25 (24):23736–23747

Wang S, Liu H, Zhang Y, Xin H (2015) The effect of CuO NPs on reactive oxygen species and cell cycle gene expression in roots of rice. Environ Toxicol Chem 34(3):554–561

Wang X, Li B, Ma Y, Hua L (2010) Development of a biotic ligand model for acute zinc toxicity to barley root elongation. Ecotoxicol Environ Saf 73(6):1272–1278

Xiang L, Zhao HM, Li YW, Huang XP, Wu XL, Zhai T, Yuan Y, Cai QY, Mo CH (2015) Effects of the size andmorphology of zinc oxide nanoparticles on the germination of Chinese cabbage seeds. Environmental Science and Pollution Research 22 (14):10452–10462

Xiong T, Dumat C, Dappe V, Vezin H, Schreck E, Shahid M, Pierart A, Sobanska S (2017) Copper oxide nanoparticle foliar uptake, phytotoxicity, and consequences for sustainable urban agriculture. Environ Sci Technol 51:5242–5251

Xiong Y, Contento AL, Bassham DC (2007) Disruption of autophagy results in constitutive oxidative stress in Arabidopsis. Autophagy 3(3):257–258

Xu Y, Wang C, Hou J, Dai S, Wang P, Miao L, Lv B, Yang Y, You G (2016) Effects of ZnO nanoparticles and Zn^{2+} on fluvial biofilms and the related toxicity mechanisms. Sci Total Environ 544:230–237

Yadav SK (2010) Heavy metals toxicity in plants: an overview on the role of glutathione and phytochelatins in heavy metal stress tolerance of plants. South Afr J Bot 76(2):167–179

Zhang D, Hua T, Xiao F, Chen C, Gersberg RM, Liu Y, Stuckey D, Ng WJ, Tan SK (2015a) Phytotoxicity and bioaccumulation of ZnO nanoparticles in *Schoenoplectus tabernaemontani*. Chemosphere 120:211–219

Zhang R, Zhang H, Tu C, Hu X, Li L, Luo Y, Christie P (2015b) Phytotoxicity of ZnO nanoparticles and the released Zn(II) ion to corn (*Zea mays L.*) and cucumber (*Cucumis sativus L.*) during germination. Environ Sci Pollut Res 22(14):11109–11117